

Computational Analysis of Elastically Supported Functionally Graded Plates with Plate Thickness Ratio and Materials Properties Having Rectangular Holes for Post Deforming in Thermal Environments

Rajesh Kumar*

NIMS University Jaipur-303121, Rajasthan, India

*Correspondence to:

Rajesh Kumar

NIMS University, Jaipur, Rajasthan, India.

E-mail: rajeshtripathi63@gmail.com

Received: November 24, 2022

Accepted: April 17, 2023

Published: April 19, 2023

Citation: Kumar R. 2023. Computational Analysis of Elastically Supported Functionally Graded Plates with Plate Thickness Ratio and Materials Properties Having Rectangular Holes for Post Deforming in Thermal Environments. *NanoWorld* J9(S1): S316-S321.

Copyright: © 2023 Kumar. This is an Open Access article distributed under the terms of the Creative Commons Attribution 4.0 International License (CCBY) (<http://creativecommons.org/licenses/by/4.0/>) which permits commercial use, including reproduction, adaptation, and distribution of the article provided the original author and source are credited.

Published by United Scientific Group

Abstract

Computational simulation of FGM (Functionally graded material) plates on foundations with rectangular holes for post deforming in thermal environments are investigated. MATLAB code, stochastic finite element, and FOPT applied for various geometric parameters to find out mean post deforming thermal load and coefficient of variations of post deforming thermal load. The variations in plate thickness ratios, aspect ratios, and power index are investigated along with variations in amplitude ratios. Present HSDT with FOPT is applied for mean post deforming thermal load and uncertainty (COV) of post deforming thermal load parameters and compared for validation with those available literatures analytical method results. There are many applications of these plates in modern life and technology used in aviation industry, Aerospace applications. Table 1 and Table 2 results are for comparison and validation purposes, Table 3, Table 4, Table 5 and Table 6 results are findings useful for further research reference. Figure 1 is the geometry of quarter plate with rectangular hole and Figure 2 presents the comparison of SD/ Mean with uncertain parameters studied in this research paper.

Keywords

Functionally graded materials plates, Uncertain parameters, Elastic supports, Rectangular holes

Introduction

TFGMs plates with rectangular cutouts are used in applications. Previous research is carried out by the researchers on the subject as analytical studies. Notably among them are Shen [1-3], Huang and Shen [4], Yang et al. [5], Wu et al. [6], and Lal et al. [7]. Some other researchers like Pandey et al. [8], Rekha et al. [9], and Komur et al. [10] studied the plate with cutouts.

It is clear that work related to computational analysis of elastically supported functionally graded plates with plate thickness ratio and materials properties having rectangular holes for post deforming in thermal environments has not been investigated in thermal environments using Stochastic finite element method.

In this paper, computational analysis is carried out of FGM plates having variations in plate thickness ratio, aspect ratios, power index, and different materials properties having rectangular holes for post deforming in thermal environments. Stochastic FEM in MATLAB is applied for investigation. The present HSDT results obtained for mean post deforming thermal load are compared and validated with published analytical results and for uncertainty (COV) of post deforming thermal load with independent MCS.

Materials and Methods

IFGM plates are supported whose load displacement relation is expresses as:

$$P = K_1 w - K_2 \nabla^2 w \quad (1)$$

For solution $\pi_1 + \pi_2 + \pi_3 + \pi_4$ with respect to the generalized displaced vector $\{q\}$ (2)
Eigen value solution of given problems is as:

$$K_o = K_b + K_s, [K_o] \{q\} = [F_t]$$

$$[[K_o] + \lambda [K_g]] = 0 \quad (3)$$

Comparative study average deforming (validation of present study)

Table 1 shows that critical buckling load obtained for same rectangular plate under biaxial loading condition is exactly half that of uniaxial loading condition. Present HSDT results are validated with Ghannadpour et al. [11] and Wadhonkar et al. [12].

Table 2 presents [HSDT] investigations are carried out for the purpose of validation. The laminates $[0, 90]_2s$ is considered. The eight layered thickness. It is noticed that present results are validated with Ghannadpour et al. analytical [11].

Geometry, modeling, and study factors

Rectangular plate material properties and geometric properties are expressed as Lal et al. [14]. The laminates are 0.15 mm thick. Higher order shear deformation theory is applied as given in [17].

Validity for random deformation

Figure 2 presents a comparative graph for SD/Mean with uncertainty in material qualities of present is compared with those published [5] and HSDT stochastic approach in conjunction with FOPT, Lal et al. [13].

Results and Discussion

MATLAB [R2010a] coding is done for rectangular holes [10]. A C0 element continuity is expressed in [11]. (Uncertainty at beginning) equal to 0.1 is expressed elaborately in [12, 13].

$$N_{cr}^* = \frac{N_x b^2}{E_2 h^3}, \lambda_{cr} = \frac{N_{cr} a^2}{\pi^2 D_0}$$

Table 2: Comparison of present [HSDT] mean buckling load (Nxb_2/E_2h^3) with semi-analytical buckling load of elliptical cutout.

d/b	e/b	Buckling load (Nxb_2/E_2h^3)	
		Ghannadpour et al. [11]	Investigated Results
0.0	0.0	13.79	13.88
0.5	0.05	13.11	13.40
0.5	0.10	12.19	12.37
0.5	0.15	11.32	11.43
0.5	0.20	10.49	10.53
0.5	0.25	9.70	9.66

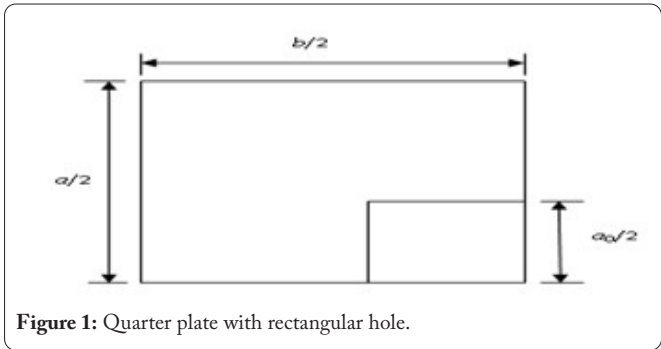


Figure 1: Quarter plate with rectangular hole.

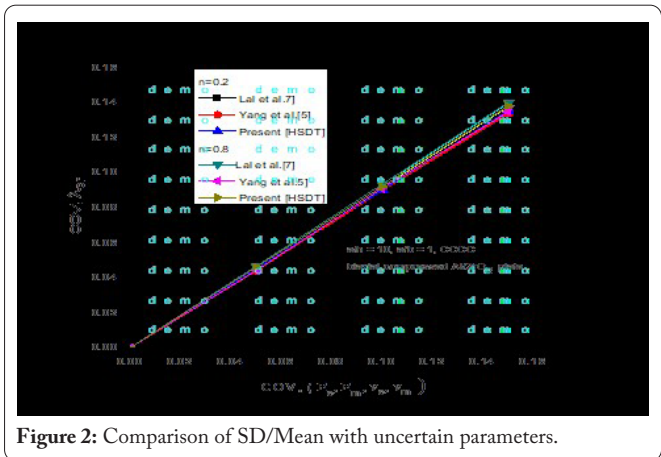


Figure 2: Comparison of SD/Mean with uncertain parameters.

Where, $D_0 = \frac{E_c h^3}{12(1-\nu_c^2)}$, $\lambda_{Tcr} = \lambda_{cr} * \alpha_0 * T \times 10^3$, and

$$K_1 = k_1 * D_{11} / a^4, K_2 = k_2 * D_{11} / a^2$$

Table 1: Comparison of present [HSDT] mean buckling load (Nxb_2/E_2h^3) with semi-analytical buckling load without cutout uniaxial and biaxial for the plate. The properties of the material of the lamina are given as $E_1 = 130.0$ GPa, $E_2 = E_3 = 10.0$ GPa, $G_{12} = G_{13} = 5.0$ GPa, $\nu_{12} = \nu_{13} = 0.35$, $\nu_{23} = \nu_{32} = 0.49$. Stacking sequence is varied mentioned below.

Stacking Sequence	Without cutout Uniaxial			Without cutout Biaxial	
	Wadhonkar et al. [12]	Ghandapour et al. [11]	Present [HSDT]	Wadhonkar et al. [12]	Present [HSDT]
(0/90)2s	16.54	16.55	16.8619	8.27	8.3550
[30/-30]2S	23.37	23.16	23.8519	11.684	11.8503
(45/-45)2s	25.65	25.92	25.7946	12.826	12.5792

Table 3: Plate studied for mean thermal postbuckling load and COV of thermal postbuckling load with rectangular cutouts, TID material properties, plate thickness ratio (a/h) = 20, plate aspect ratio (a/b) = 1, plate dimensions length (a) = 50), (width b) = 50). Elliptical cutout for varying power Index (n), amplitude ratios (W_{max}/h = 0.0 - 1.0), Foundation parameters.

a/b	n	W_{max}/h	Rectangular Hole					
			$(k_1 = 0, k_2 = 0)$		$(k_1 = 100, k_2 = 0)$		$(k_1 = 100, k_2 = 10)$	
			Average	SD/Mean	Average	SD/Mean	Average	SD/Mean
20	0.0	0.0	0.9702	0.1009	1.0093	0.1009	1.1244	0.1008
		0.5	1.0784	0.0946	1.1171	0.0949	1.2269	0.0956
		1.0	1.1674	0.1020	1.1978	0.1027	1.3162	0.1013
	0.5	0.0	0.6453	0.0880	0.6843	0.0888	0.7986	0.0901
		0.5	0.7244	0.0821	0.7626	0.0832	0.7992	0.0967
		1.0	0.8635	0.1136	0.9099	0.0911	1.0060	0.1139
	1.0	0.0	0.5014	0.0856	0.5403	0.0859	0.6537	0.0865
		0.5	0.5671	0.0787	0.6035	0.0798	0.7140	0.0817
		1.0	0.6624	0.1078	0.6040	0.0863	0.7282	0.0871
	2.0	0.0	0.3884	0.0979	0.4269	0.0947	0.5387	0.0892
		0.5	0.4390	0.0880	0.4751	0.0867	0.5845	0.0838
		1.0	0.9941	0.2738	0.4941	0.1011	1.0230	0.2029
	5.0	0.0	0.3118	0.0925	0.3496	0.0880	0.4590	0.0814
		0.5	0.3471	0.0844	0.3829	0.0818	0.4908	0.0775
		1.0	0.3551	0.0847	0.4212	0.0883	0.5448	0.0790
	10.0	0.0	0.2765	0.0806	0.3139	0.0774	0.4217	0.0738
		0.5	0.3047	0.0751	0.3405	0.0733	0.4473	0.0711
		1.0	0.3810	0.0683	0.3999	0.0773	0.4897	0.0734

Table 4: Plate studied for mean thermal postbuckling load and COV load with elliptical cutouts, TID material properties, Plate thickness ratio (a/h) = 10, plate aspect ratio (a/b) = 1, Plate dimensions length (a) = 50), (Width b) = 50). Rectangular cutout CCCC support for varying power index (n), Amplitude ratios (W_{max}/h = 0.0 - 1.0).

n	W_{max}/h	Rectangular Cutout ($a_0/b_0 = 1.5$)					
		$(k_1 = 0, k_2 = 0)$		Support 1		Support 2	
		Mean	COV	Mean	COV	Mean	COV
0.0	0.0	5.5275	0.1007	5.8028	0.1008	6.6421	0.1005
	0.5	6.3331	0.0923	6.6022	0.0929	7.4448	0.0943
	1.0	6.3532	0.1062	6.8320	0.1092	7.2662	0.1079
0.5	0.0	3.7142	0.0883	3.9912	0.0893	4.8231	0.0909
	0.5	4.2852	0.0808	4.5857	0.0820	5.1562	0.0898
	1.0	4.8242	0.1387	5.0222	0.1395	5.6085	0.1281
1.0	0.0	2.8937	0.0844	3.1696	0.0851	3.9915	0.0863
	0.5	3.3769	0.0757	3.6536	0.0775	4.3776	0.0968
	1.0	3.7257	0.1239	4.9186	0.2771	6.1595	0.1915
2.0	0.0	2.2279	0.0917	2.4975	0.0886	3.2990	0.0848
	0.5	2.2315	0.0813	2.8268	0.0810	3.4301	0.0847
	1.0	2.8958	0.1166	3.0246	0.1127	3.6959	0.1057
5.0	0.0	1.7372	0.0858	1.9883	0.0811	2.7499	0.0764
	0.5	1.7598	0.0865	2.1569	0.0916	2.8975	0.0752
	1.0	2.1466	0.1055	2.2553	0.0800	3.2135	0.1343
10.0	0.0	1.5227	0.0793	1.7625	0.0758	2.5014	0.0720
	0.5	1.7240	0.0728	1.8672	0.0831	2.5256	0.0732
	1.0	1.9553	0.1202	1.8726	0.0853	2.5829	0.0781

Where, $D_{11} = (E_2 * b^3) / (12) * (1 - \nu_{12}^2)$

Where, λ_{cr} and λ_{Tcr} are dimensionless parameters of plate and materials Al/ZrO₂ and Al/Al₂O₃.

$\lambda_{cr} = N_{cr} * \alpha_c * \Delta T * 1000$

Table 3, it is noticed that for same plate thickness ratio on increasing volume fraction index the mean and COV decreases, however on increasing amplitude ratio increase for plate supports. On further increasing the plate thickness ratio the mean and COV further decrease to lower values, however it is higher for supports.

Table 4, it is seen that for given power index the expected mean and COV of thermal postbuckling load increase on increasing amplitude ratios for plate without and with Winkler and Pasternak elastic foundations. However, these values further decrease on increase of volume fraction index. It means on increase of power index the buckling tendency increases for given temperature in present study.

Table 5, it is seen that for same aspect ratio on increasing

volume fraction index the mean and COV of thermal post-buckling load decreases. However, on increasing amplitude ratio for plate on support, thermal postbuckling load increases. It is higher for support. On further increasing the aspect ratio the Mean and COV further increase to higher values, however it is higher for supports COV for volume fraction index (0.5) is much higher than other so this must be avoided for design purpose.

Table 6, it is seen that for SSSS support and Al/ZrO₂ plate material, on increasing minor axis values the Mean and COV of thermal postbuckling load increases, however on increasing amplitude ratio increase for plate supported. It is higher for support. On change to Al/Al₂O₃ plate material.

Table 5: Plate studied for mean thermal postbuckling load COV postbuckling load with elliptical cutouts, (a/h = 30). Plate dimensions length (a = 50), (Width b = 50). Rectangular cutout (a₀/b₀ = 1.5) for varying plate aspect ratio (a/b), power index (n).

a/b	n	W _{max} /h	Rectangular Cutout					
			(k ₁ = 0, k ₂ = 0)		Support 1		Support 2	
			Mean	COV	Mean	COV	Mean	COV
1	0.0	0.0	0.3388	0.1010	0.3504	0.1010	0.3852	0.1008
		0.5	0.3722	0.0956	0.3828	0.0960	0.4172	0.0963
		1.0	0.4490	0.0914	0.4320	0.0983	0.4925	0.0940
	0.5	0.0	0.2249	0.0879	0.2364	0.0885	0.2707	0.0898
		0.5	0.2492	0.0830	0.2601	0.0839	0.2937	0.0859
		1.0	0.3204	0.0758	0.3295	0.0804	0.3442	0.0871
	1.0	0.0	0.1747	0.0860	0.1861	0.0862	0.2202	0.0865
		0.5	0.1945	0.0801	0.2053	0.0809	0.2389	0.0823
		1.0	0.2519	0.0747	0.2587	0.0844	0.2789	0.0832
	2.0	0.0	0.1356	0.0995	0.1469	0.0967	0.1806	0.0912
		0.5	0.1508	0.0909	0.1614	0.0893	0.1950	0.0859
		1.0	0.1951	0.0820	0.1960	0.0849	0.2246	0.0843
	5.0	0.0	0.1096	0.0944	0.1209	0.0904	0.1542	0.0836
		0.5	0.1203	0.0873	0.1310	0.0846	0.1618	0.0832
		1.0	0.1517	0.0748	0.1576	0.0771	0.1872	0.0771
	10.0	0.0	0.0975	0.0810	0.1088	0.0781	0.1418	0.0744
		0.5	0.1061	0.0763	0.1169	0.0745	0.1498	0.0719
		1.0	0.1314	0.0675	0.1411	0.0663	0.1722	0.0719
2	0.0	0.0	1.3565	0.1000	1.3586	0.1000	1.4123	0.1000
		0.5	1.6177	0.0971	1.5596	0.1041	1.6790	0.0969
		1.0	2.1326	0.0836	1.3610	0.0753	2.1496	0.0840
	0.5	0.0	1.1880	0.1086	1.1915	0.1088	1.2452	0.1082
		0.5	1.1093	0.1024	1.1135	0.1022	1.1687	0.1019
		1.0	1.2356	0.1385	0.9851	0.3208	1.2569	0.0795
	1.0	0.0	0.5882	0.5885	0.2902	1.5321	0.3373	0.3378
		0.5	1.1304	0.0717	0.3919	0.0832	0.9788	0.0730
		1.0	0.5241	0.3293	1.0957	0.7909	0.9239	0.0834
	2.0	0.0	0.5882	0.5885	0.5904	0.5717	0.6395	0.5122
		0.5	0.6077	0.2715	0.5222	0.1609	0.6743	0.1713
		1.0	0.5533	0.0376	0.5524	0.0272	0.5182	0.5900
	5.0	0.0	0.2398	0.2680	0.2428	0.2595	0.2904	0.2247
		0.5	0.1820	0.4748	0.2172	0.3176	0.2341	0.3689
		1.0	0.1144	0.6532	0.3470	0.0642	0.0405	0.2565
	10.0	0.0	0.1340	0.4609	0.1373	0.4432	0.1843	0.3257
		0.5	0.0719	0.1892	0.0746	1.1274	0.1315	0.5716
		1.0	0.2114	0.2510	0.2122	0.2607	0.6550	0.0968

Table 6: Plate studied for mean thermal postbuckling load and COV postbuckling load with elliptical cutouts, TID material properties, rectangular cutouts, TID material properties, $a/h = 20$, $n = 5.0$, (a_0/b_0) for $(a_0 = 0, 2.5, 5, 7.5, 10, 12.5, \text{ and } b_0 = 25)$ for different type of materials (Al/ZrO_2) , (Al/Al_2O_3) , variations in aspect ratios, Amplitude ratios $(W_{max}/h = 0.0 - 1.0)$.

Type of material	a_0/b_0	W_{max}/h	Rectangular Cutout					
			$(k_1 = 0, k_2 = 0)$		Support 1		Support 2	
			Mean	COV	Mean	COV	Mean	COV
Al/ZrO ₂	0.0	0.0	0.6719	0.0754	0.7158	0.0736	0.8425	0.0722
		0.5	0.7209	0.0870	0.7605	0.0836	0.8822	0.0781
		1.0	0.8685	0.1092	0.8968	0.1054	0.9990	0.0954
	0.1	0.0	0.9375	0.0754	0.9674	0.0735	1.0889	0.0720
		0.5	1.0210	0.0742	1.0446	0.0721	1.1573	0.0703
		1.0	1.2688	0.0726	1.2595	0.0715	1.2489	0.0734
	0.2	0.0	0.9905	0.0754	1.0040	0.0736	1.1086	0.0717
		0.5	1.0795	0.0736	1.0864	0.0717	1.1819	0.0698
		1.0	1.3436	0.0701	1.3193	0.0692	1.3203	0.0717
	0.3	0.0	1.0481	0.0754	1.0446	0.0737	1.1324	0.0716
		0.5	1.1430	0.0731	1.1323	0.0714	1.2098	0.0695
		1.0	1.4264	0.0684	1.3868	0.0674	1.4420	0.0658
	0.4	0.0	1.1139	0.0754	1.0932	0.0739	1.1642	0.0715
		0.5	1.2155	0.0727	1.1864	0.0713	1.2467	0.0693
		1.0	1.5206	0.0670	1.4637	0.0661	1.4903	0.0647
	0.5	0.0	1.1896	0.0754	1.1514	0.0741	1.2059	0.0715
		0.5	1.2982	0.0724	1.2505	0.0712	1.2928	0.0691
		1.0	1.6270	0.0660	1.5551	0.0652	1.5642	0.0638
Al/Al ₂ O ₃	0.0	0.0	0.5615	0.1001	0.6122	0.0910	0.5800	0.0825
		0.5	0.6044	0.1173	0.6495	0.1068	0.6042	0.0917
		1.0	0.7341	0.1315	0.7602	0.1235	0.6740	0.1044
	0.1	0.0	0.7841	0.0972	0.8193	0.0898	0.7481	0.0824
		0.5	0.8577	0.0941	0.8831	0.0870	0.7890	0.0803
		1.0	1.0751	0.0858	0.9623	0.0858	0.8326	0.0796
	0.2	0.0	0.8283	0.0966	0.8398	0.0899	0.7485	0.0823
		0.5	0.9068	0.0924	0.9080	0.0863	0.7922	0.0798
		1.0	1.1392	0.0823	1.0937	0.0802	0.8740	0.0792
	0.3	0.0	0.8763	0.0959	0.8636	0.0901	0.7523	0.0822
		0.5	0.9600	0.0909	0.9360	0.0858	0.7982	0.0794
		1.0	1.2063	0.0552	1.1550	0.0761	0.8733	0.0791
	0.4	0.0	0.9309	0.0952	0.8937	0.0903	0.7614	0.0823
		0.5	1.0198	0.0898	0.9707	0.0856	0.8096	0.0792
		1.0	1.2900	0.0774	1.1883	0.0771	0.9474	0.0735
	0.5	0.0	0.9936	0.0947	0.9318	0.0905	0.7769	0.0825
		0.5	1.0888	0.0887	1.0155	0.0851	0.8278	0.0790
		1.0	1.3797	0.0756	1.4597	0.1021	0.9863	0.0713

Conclusion

Computational analysis of elastically supported FGM plates with rectangular cutouts for post deforming in thermal environments is carried out. Thermal postbuckling load of FGM plate subjected to uniaxial compression decreases. In the rectangular cutouts, one which aligned perpendicular to load direction represents higher buckling load than one aligned in. It concludes that when plates with rectangular cutouts are supported, postbuckling is at higher temperature for same properties compared to without foundations. This parameter is one of the other important parameters while considering plates with rectangular cut out because thermal stresses are more in cutout section.

Acknowledgements

None.

Conflict of Interest

Author assures no conflict of interests are relevant to the content of this article.

Credit Author Statement

Rajesh Kumar: Conceptualization, Methodology, Investigation, Data analysis, Writing - original draft preparation, Writing - review and editing. The author read and approved the manuscript.

References

1. Shen HS. 2000. Hygrothermal effects on the postbuckling of composite laminated cylindrical shells. *Compos Sci Technol* 60(8): 1227-1240. [https://doi.org/10.1016/S0266-3538\(00\)00062-2](https://doi.org/10.1016/S0266-3538(00)00062-2)
2. Shen HS. 2001. The effects of hygrothermal conditions on the post-buckling of shear deformable laminated cylindrical shells. *Int J Solids Struct* 38(36-37): 6357-6380. [https://doi.org/10.1016/S0020-7683\(01\)00123-8](https://doi.org/10.1016/S0020-7683(01)00123-8)
3. Shen HS. 2002. Hygrothermal effects on the postbuckling of axially loaded shear deformable laminated cylindrical panels. *Compos Struct* 56(1): 73-85. [https://doi.org/10.1016/S0263-8223\(01\)00187-8](https://doi.org/10.1016/S0263-8223(01)00187-8)
4. Huang XL, Shen HS. 2004. Nonlinear vibration and dynamic response of functionally graded plates in thermal environments. *Int J Solids Struct* 41(9-10): 2403-2427. <https://doi.org/10.1016/j.ijsolstr.2003.11.012>
5. Yang J, Liew KM, Kitipornchai S. 2005. Second-order statistics of the elastic buckling of functionally graded rectangular plates. *Compos Sci Technol* 65(7-8): 1165-1175. <https://doi.org/10.1016/j.compscitech.2004.11.012>
6. Wu TL, Shukla KK, Huang JH. 2007. Post-buckling analysis of functionally graded rectangular plates. *Compos Struct* 81(1): 1-10. <https://doi.org/10.1016/j.compstruct.2005.08.026>
7. Lal A, Kulkarni NM, Singh BN. 2015. Stochastic thermal post buckling response of elastically supported laminated piezoelectric composite plate using micromechanical approach. *Curved Layer Struct* 2(1): 331-350. <https://doi.org/10.1515/cls-2015-0019>
8. Pandey R, Upadhyay AK, Shukla KK. 2010. Hygrothermoelastic post-buckling response of laminated composite plates. *J Aerosp Eng* 23(1): 1-13. [https://doi.org/10.1061/\(ASCE\)0893-1321\(2010\)23:1\(1\)](https://doi.org/10.1061/(ASCE)0893-1321(2010)23:1(1))
9. Rekha S, Tushar S, Rajendra B. Effect of various cut out on buckling analysis of laminated composite plate using FEM simulation. *ELK Asia Pacific J* 978-81-930411-4-7 <https://doi.org/10.16962/elkajp/si.arimpic-2015.12>
10. Komur MA, Sen F, Ataş A, Arslan N. 2010. Buckling analysis of laminated composite plates with an elliptical/circular cutout using FEM. *Adv Eng Softw* 41(2): 161-164. <https://doi.org/10.1016/j.advengsoft.2009.09.005>
11. Shankara CA, Iyengar NGR. 1996. A C⁰ element for the free vibration analysis of laminated composite plates. *J Sound Vib* 191(5): 721-738. <https://doi.org/10.1006/jsvi.1996.0152>
12. Kleiber M, Hien TD. 1992. *The Stochastic Finite Element Method*. Wiley, New York.
13. Yimin Z, Chen S, Liu Q, Liu T. 1996. Stochastic perturbation finite elements. *Comp Struct* 59(3): 425-429. [https://doi.org/10.1016/0045-7949\(95\)00267-7](https://doi.org/10.1016/0045-7949(95)00267-7)
14. Lal A, Jagtap KR, Singh BN. 2013. Post buckling response of functionally graded materials plate subjected to mechanical and thermal loadings with random material properties. *Appl Math Model* 37(5): 2900-2920. <https://doi.org/10.1016/j.apm.2012.06.013>
15. Ghannadpour SAM, Najafi A, Mohammadi B. 2006. On the buckling behavior of cross-ply laminated composite plates due to circular/elliptical cutouts. *Compos Struct* 75(1-4): 3-6. <https://doi.org/10.1016/j.compstruct.2006.04.071>
16. Wadhonkar S, Kadam K. 2017. Bucking analysis of laminated composite plates with cut-out. *Int J Innov Res Sci Eng Technol* 6(1):423-427.
17. Reddy JN. 1984. A simple higher-order theory for laminated composite plates. *J Appl Mech* 51(4): 745-752. <https://doi.org/10.1115/1.3167719>